

Journal of Intelligent Material Systems and Structures

<http://jim.sagepub.com/>

Use of grey relational analysis for multi-objective optimisation of NiTiCu shape memory alloy produced by powder metallurgy process

Alireza Sadeghi, Abolfazl Babakhani, Seyed Mojtaba Zebarjad and Hassan Mostajabodaveh

Journal of Intelligent Material Systems and Structures 2014 25: 2093 originally published online 13 January 2014

DOI: 10.1177/1045389X13517312

The online version of this article can be found at:

<http://jim.sagepub.com/content/25/16/2093>

Published by:



<http://www.sagepublications.com>

Additional services and information for *Journal of Intelligent Material Systems and Structures* can be found at:

Email Alerts: <http://jim.sagepub.com/cgi/alerts>

Subscriptions: <http://jim.sagepub.com/subscriptions>

Reprints: <http://www.sagepub.com/journalsReprints.nav>

Permissions: <http://www.sagepub.com/journalsPermissions.nav>


Citations: <http://jim.sagepub.com/content/25/16/2093.refs.html>

>> [Version of Record](#) - Sep 26, 2014

[OnlineFirst Version of Record](#) - Jan 13, 2014

[What is This?](#)

Use of grey relational analysis for multi-objective optimisation of NiTiCu shape memory alloy produced by powder metallurgy process

Journal of Intelligent Material Systems and Structures
2014, Vol. 25(16) 2093–2101
© The Author(s) 2014
Reprints and permissions:
sagepub.co.uk/journalsPermissions.nav
DOI: 10.1177/1045389X13517312
jim.sagepub.com


Alireza Sadeghi¹, Abolfazl Babakhani², Seyed Mojtaba Zebarjad² and Hassan Mostajabodaveh²

Abstract

Powder metallurgy process was used in this work to produce NiTi specimens. Uniaxial compression, X-ray diffraction and differential scanning calorimetry were used for characterising the produced samples. L9 orthogonal arrays were chosen based on the Taguchi method for conducting the experiments. In order to optimise the processing parameters and also to determine the level of importance of each parameter, experiments were performed based on grey relational method. Our goal was to optimise recoverable strain (ϵ) and the finishing temperature of austenitic transformation (A_f). Sintering time, compaction pressure, milling time and the atomic percentage of Cu were all selected as controllable parameters. Our results reveal that the sintering time and the atomic percentage of Cu are the most significant parameters. The findings were verified through a confirmatory test.

Keywords

Powder metallurgy, nitinol, shape memory, grey relational analysis, optimisation

Introduction

Currently, NiTi alloys are known as effective biomaterials for orthopaedic, dental and cardiovascular applications. These alloys have valuable characteristics, such as shape memory effect, super-elasticity, corrosion resistance, wear resistance and biocompatibility (Arciniegas et al., 2007; Chu et al., 2004; Maziarz et al., 2004).

Some current methods for producing the practically used NiTi alloys are vacuum induction melting and electric arc melting. Segregation formation, crucible contamination absorption and gas absorption are conventional problems of producing NiTi alloys by these methods; in addition, producing complex shapes is difficult with these methods (Elahinia et al., 2012).

In recent years, there have been numerous investigations on the use of conventional powder metallurgy (PM) techniques to produce porous NiTi alloys. The PM techniques are good candidates for producing near net-shape components due to the potential to utilise lesser volume of precursor materials (Bram et al., 2002). Moreover, the PM methods allow for the exact control of the chemical composition (Chung et al., 2004).

Formation of NiTi in PM processing is not favoured in primary reactions between Ni and Ti due to prevailing thermodynamic conditions. Thus, NiTi is obtained as a product of secondary reactions involving primary reaction products of NiTi₂ and Ni₃Ti (Neves et al., 2011).

Some of the PM methods are as follows: self-propagating high temperature synthesis (SHS) (Chu et al., 2004; Chung et al., 2004), conventional pressing and sintering of the powder (Li et al., 1998; Zhang et al., 1992), hot isostatic pressing (HIP) (Lagoudas and Vandygriff, 2002; McNeese et al., 2000), metal injection moulding (Guoxin et al., 2008; Schöller et al., 2005), sintering in reduction atmosphere (Zhu et al.,

¹Materials Research Group, Iranian Academic Center for Education, Culture and Research (ACECR), Mashhad, Iran

²Department of Materials and Metallurgical Engineering, School of Engineering, Ferdowsi University of Mashhad, Mashhad, Iran

Corresponding author:

Alireza Sadeghi, Materials Research Group, Iranian Academic Center for Education, Culture and Research (ACECR), Mashhad Branch, P.O. Box 91775-1376, Azadi Square, Mashhad, Iran.
Email: Sadeghi_av@ymail.com

2004), vacuum sintering (Khalifehzadeh et al., 2007), spark plasma sintering (Zhao et al., 2005) and mechanical alloying (MA) (Pilarczyk et al., 2011; Sadrnezhaad and Selahi, 2004). Among these, researchers have focused mainly on SHS, HIP and sintering in vacuum or a reduction atmosphere for producing NiTi shape memory alloys. Inability to control the intermetallic phases is one drawback of SHS method, and usually Ti_2Ni , Ni_3Ti and Ni_4Ti_3 precipitates are present in the matrix of SHS products (Lagoudas and Vandygriff, 2002); costly equipment and probability of creation of secondary phases are some difficulties of HIP method (Elahinia et al., 2012) and limitation in shape and pore size of samples, long heating times and undesirable secondary phases are some difficulties of conventional sintering (Elahinia et al., 2012).

For biomaterial applications, the elastic modulus of implants produced via PM can be made closer to the modulus of bone, and this can eliminate the problems associated with stress-shielding phenomena in conventional metallic implants. Moreover, enhanced fixation can be achieved by improving the bone tissue growth throughout the porous matrix of these implants (Ryan et al., 2006).

Use of copper as a ternary alloying element results in increase in the martensitic transformation temperature. Also, copper has good corrosion resistance, less composition sensitivity of martensitic start temperature (M_s) and narrow transformation hysteresis, but an addition of more than 10 at % reduces alloy formability (Goryczka and Van Humbeeck, 2008).

There are limited works about producing ternary NiTiCu shape memory alloys by PM methods. For instance, Goryczka and Van Humbeeck (2008) produced $Ni_{50-x}Ti_{50}Cu_x$ (where $x = 2, 3, 5, 10, 15, 20, 25$ at %) by powder technology. They tried various conditions for sintering and concluded that a homogeneous alloy can be obtained only by correct combination of sintering temperature and time (for copper less than 5 at%, it was 940 °C for 7 h; for copper more than 10 at%, it was 850 °C for 20 h). Terayama and Kyogoku (2010) fabricated $Ni_{50.2-x}TiCu_x$ ($x = 0, 5, 10, 15, 20$ mol%) alloy by MA of elemental powders; they investigated shape memory characteristics, phase transformation behaviour and also thermo-mechanical properties of the produced alloys.

The PM process is affected by many different parameters, such as the material composition, size and purity of the primary powders, milling time and milling speed, sintering time and sintering temperature and compaction pressure. Due to the large number of input parameters, design of experiments (DOEs) based on the Taguchi method can be very useful for saving time and cost. This issue has gained little attention in other works. Additionally, in medical applications, it is ideal to have a NiTi alloy with transformation temperature around the body temperature for good shape memory

function. Therefore, the objective of this work was to maximise both A_f and ε to determine the optimal parameter combination and the level of importance of each parameter for processing. Since the traditional Taguchi method cannot solve a multi-objective optimisation, a grey relational analysis (GRA) was used to overcome this problem.

Materials and methods

Raw materials and powder processing

Elemental powders of titanium (mean particle size: $\sim 650 \mu m$, purity: 99.5%), nickel (mean particle size: $\sim 10 \mu m$, purity: 99.8%) and copper (mean particle size: $\sim 60 \mu m$, purity: 98%) were mixed at room temperature for producing $Ni_{50-x}Ti_{50}Cu_x$ specimens with different atomic percentage of Cu (0, 5, 10). Mixing was performed on a planetary ball mill with stainless steel vial (1500 mL in volume) and two different sizes of stainless steel balls (8 and 10 mm in diameter) without the addition of a process control agent. The ball-to-powder weight ratio and the milling speed were kept at 40:1 and 300 r/min, respectively. The maximum milling time was 54 h. The vial was evacuated and filled with high-purity argon gas (99.99%) during the mixing. The cylindrical preforms with a size of 10 mm in diameter and 20 mm in height were obtained by a uniaxial cold compaction under different pressures (600, 750 and 900 MPa). Then, sintering was carried out under pure argon atmosphere (99.99%) at 1050 °C for various times (4, 7 and 10 h), and finally after sintering, the specimens aged at 500 °C for 0.5 h in an argon atmosphere and then quenched in water.

Characterisation

The phase constituents of the specimens were determined by X-ray diffraction (XRD). X-ray diffractometer Philips PW1140 was used at room temperature with Cu K_α radiation ($\lambda = 0.1541874$ nm) at a voltage and electrical current of 40 kV and 30 mA, respectively. To study the stress-strain behaviour of the samples, uniaxial compression tests were performed at room temperature at a rate of 0.2 mm/min on a Zwick (Z 250) testing machine. The strain is measured in this machine by a contact type extensometer (Type B066552). The characteristic temperatures of transformation were determined by differential scanning calorimetry (DSC) with a preheating temperature of 250 °C and a heating/cooling rate of 10 °C/min.

Experimental design

For PM processing, a high number of experiments must be carried out to determine the optimal processing conditions, as there are many parameters to consider. Use

of experimental design in such cases can be very useful. Conventional approaches for DOEs are classical (full factorial, fractional factorial, response surface methodology) and Taguchi method.

Basically, classical approaches are complicated, ineffective and frustrating for managers, engineers and workers and so those methods tended to be preferred by only those with a statistical or mathematical inclination (Tay and Butler, 1999).

In full factorial approach, all paired interactions can be studied. However, the number of runs goes up exponentially as additional factors are added. Fractional factorial design can be used to reduce the number of runs by evaluating only a subset of all possible combinations of the factors. In a large system, it usually produces an experimental design that is desired. However, random design works poorly for systems with a small number of variables (Tay and Butler, 1999).

The Taguchi method (Roy, 2010) allows for the analysis of many different parameters without a prohibitively high amount of experimentation. Taguchi method emphasises a mean performance characteristic value close to the target value rather than a value within certain specification limits, thus improving the product quality. One limitation is that the Taguchi methods are offline, and therefore inappropriate for a dynamically changing process such as a simulation study. Also, for more than three levels, the selection is limited to a maximum of six factors. Another limitation is that Taguchi method cannot solve a multi-objective optimisation.

In this work, experiments were designed and conducted based on Taguchi's orthogonal array; since the traditional Taguchi method cannot solve a multi-objective optimisation, a GRA was used to determine the optimum process parameters for multiple responses. The grey system theory (Deng, 1982, 1989) is useful for dealing with poor, incomplete and uncertain information. Optimisation of the complicated multiple performance characteristics can be converted into optimisation of a single grey relational grade.

In this study, four parameters were used as control factors with three levels of variations for each parameter (Table 1).

The control factor levels were selected according to our primary experiences, and some parameters, such as purity, the particle size of the primary elemental

powders, ball milling speed and sintering temperature, were considered as noise factors and kept constant during experimentation. As shown in Table 2, L_9 orthogonal arrays were chosen based on the Taguchi method.

Optimisation

In this method, the following steps are followed for optimisation using GRA (Deng, 1989):

1. Grey relational generation

In the first step, the experimental results are normalised in a range from 0 to 1 (Table 3).

In this study, normalisation was computed for the 'larger-the-better' type of response according to equation (1)

$$x_i(k) = \frac{y_i(k) - \min y_i(k)}{\max y_i(k) - \min y_i(k)} \quad (1)$$

In the above equation, $x_i(k)$ are the normalised data (Table 3), $y_i(k)$ is the k th response of the i th experiment, $\min y_i(k)$ is the minimum value in the original sequence and $\max y_i(k)$ is the maximum value in the original sequence.

2. Grey relational coefficient

The grey relational coefficient is calculated according to equation (2)

$$\xi_i(k) = \frac{\Delta_{\min} + \xi \Delta_{\max}}{\Delta_{oi}(k) + \xi \Delta_{\max}} \quad (2)$$

Here, $\Delta_{oi}(k)$ is the deviation sequence of the reference sequence according to equation (3)

$$\Delta_{oi}(k) = \|x_o(k) - x_i(k)\| \quad (3)$$

In the above equation, $\|x_o(k) - x_i(k)\|$ is the absolute of the difference between $x_o(k)$ and $x_i(k)$, and $x_o(k)$ is the ideal or reference sequence. Also, Δ_{\min} and Δ_{\max} are defined as

$$\Delta_{\min} = \min_{\forall j \in i} \min_{\forall k} \|x_o(k) - x_j(k)\| \quad (4)$$

$$\Delta_{\max} = \max_{\forall j \in i} \max_{\forall k} \|x_o(k) - x_j(k)\| \quad (5)$$

Table 1. Input parameters and their levels.

Processing parameter	Symbol	Level 1	Level 2	Level 3
Milling time (h)	A	36	20	54
Compaction pressure (MPa)	B	600	750	900
Sintering time (h)	C	7	10	4
Cu (at.%)	D	0	5	10

Table 2. Experimental design using a L_9 orthogonal array.

Test no.	Milling time (h)	Compaction pressure (MPa)	Sintering time (h)	Cu (at.%)	ε (%)	A_f
1	36	600	7	0	0.95	17.2
2	36	750	10	5	1.07	21.1
3	36	900	4	10	1.22	27
4	20	600	10	10	1.45	32
5	20	750	4	0	0.75	8
6	20	900	7	5	1.2	33
7	54	600	4	5	0.78	21.9
8	54	750	7	10	1.1	39.6
9	54	900	10	0	0.85	24.3

Table 3. Data preprocessing for each performance characteristic.

Experiment no.	ε (%)	A_f ($^{\circ}\text{C}$)
Ideal sequence	1	1
1	0.2857	0.2911
2	0.4571	0.4145
3	0.6714	0.6012
4	1	0.7594
5	0	0
6	0.6428	0.7911
7	0.0428	0.4398
8	0.5	1
9	0.1428	0.5158

Table 4. Calculated grey relational coefficient for each output parameter.

Experiment y	ε (%)	A_f ($^{\circ}\text{C}$)
Ideal sequence	1	1
1	0.4117	0.4135
2	0.4794	0.4606
3	0.6034	0.5562
4	1	0.6751
5	0.3334	0.3334
6	0.5832	0.7053
7	0.3431	0.4716
8	0.3334	1
9	0.3684	0.5080

The symbol ξ is the distinguishing coefficient ($\xi \in [0, 1]$).

ξ may be adjusted based on the practical needs of the system. Since both the object responses are of equal weight in this work, the value of ξ is taken as 0.5.

Results for grey relational coefficient can be seen in Table 4.

3. Grey relational grade

The grey relational grade γ_i was obtained by 'equation (6)'

Table 5. Calculated grey relational grades and orders.

Experiment no.	Grey relational grade	Order
1	0.4126	7
2	0.47	5
3	0.5798	4
4	0.83755	1
5	0.3334	9
6	0.64425	3
7	0.40735	8
8	0.6667	2
9	0.4382	6

$$\gamma_i = \frac{1}{n} \sum_{k=1}^n \xi_i(k) \quad (6)$$

Here, γ_i is the i th grey relational grade of each experiment and was obtained by averaging the grey relational coefficients. Additionally, n is the number of responses, where in this study, $n = 2$. As seen in Table 5, the results are ordered by value. Because $x_o(k)$ represents the best sequence, the higher value of the grey relational grade shows that the corresponding parameter combination is closer to the optimal setting. In this study, the fourth experiment has the highest value, indicating the best multiple performance characteristics using the combination A2B1C2D3.

The average grey relational grades for each parameter level correspond to their orthogonal array table (Table 2), as listed in Table 6. As mentioned previously, the higher value of the grey relational grade shows that the corresponding parameter combination is closer to the optimal setting, and it can be seen from Table 6 that the combination A2B3C2D3 represents the largest average response. This is the optimal parameter combination.

The difference between the maximum and minimum of the grey relational grades for each parameter is also listed in Table 6. The magnitude of this difference is related to the importance of the control parameters; more amount of this difference represents the stronger effect of parameter on the output response.

Table 6. Response table for the grey relational grades.

Processing parameters	Level 1	Level 2	Level 3	Max–min
Milling time	0.4874	0.6050	0.5040	0.1176
Compaction pressure	0.5525	0.4900	0.5540	0.064
Sintering time	0.5745	0.5819	0.4401	0.1418
Cu (at.%)	0.3947	0.5072	0.6946	0.2999

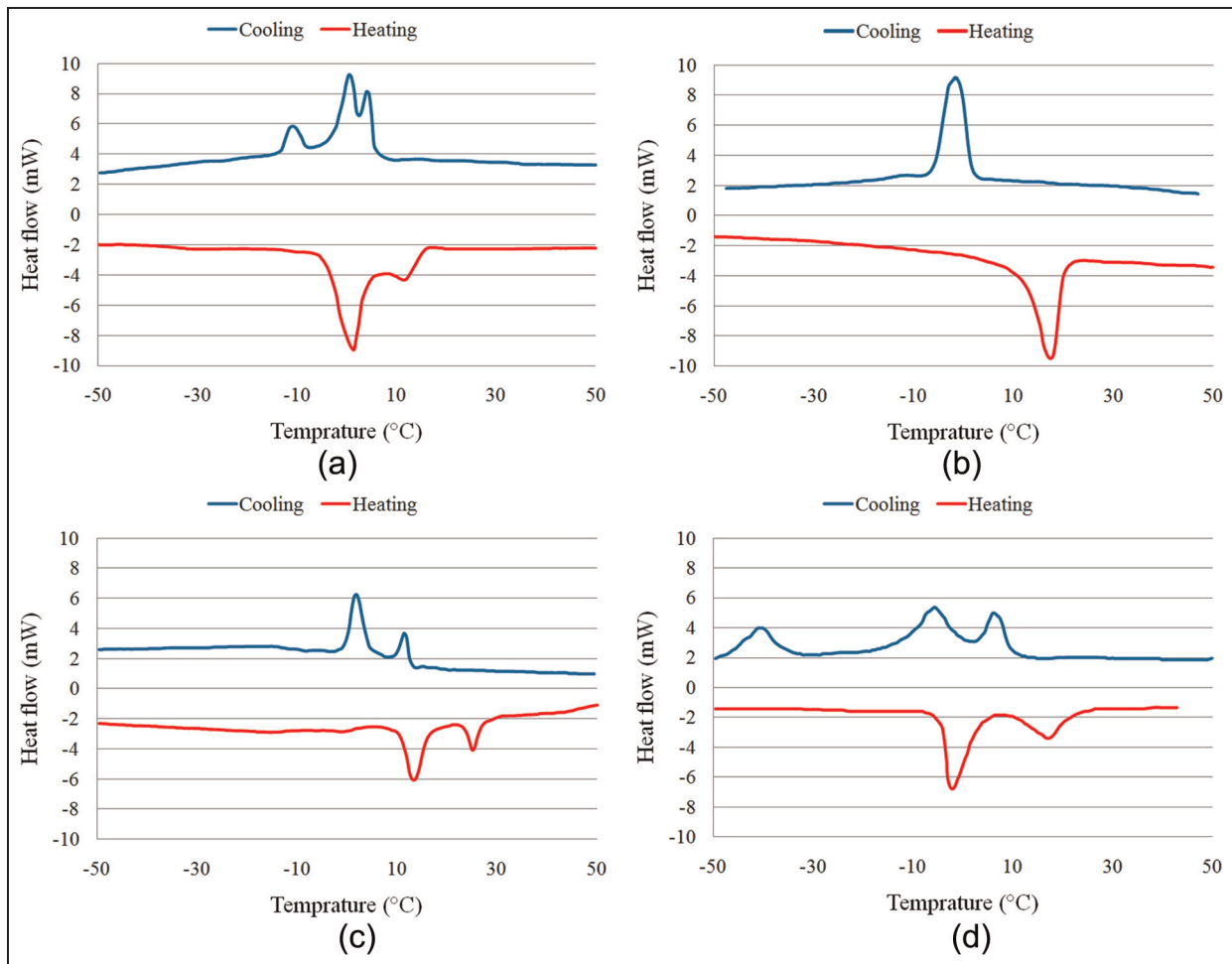


Figure 1. DSC curves of NiTi-produced samples (preheated at 250 °C, cooling/heating rate of 10 °C/min and aged at 500 °C for 0.5 h). (a) Experiment 1: milling time = 36 h, compaction pressure = 600 MPa, sintering time = 7 h and Cu (at.%) = 0. (b) Experiment 2: milling time = 36 h, compaction pressure = 750 MPa, sintering time = 10 h and Cu (at.%) = 5. (c) Experiment 3: milling time = 36 h, compaction pressure = 900 MPa, sintering time = 4 h and Cu (at.%) = 10. (d) Experiment 9: milling time = 54 h, compaction pressure = 900 MPa, sintering time = 10 h and Cu (at.%) = 0. DSC: differential scanning calorimetry.

Results and discussion

The goal of this study was to optimise the recoverable strain (ϵ) and austenitic finish temperature (A_f). The DSC curves of nine experiments during cooling cycle can be divided into three categories: curves with one peak, two peaks and three peaks. Graphs that are shown in Figure 1 include all these three types of curves, and for brevity, all graphs of experiments are not presented here.

For the first experiment, during the heating cycle, a two-stage transformation (B19'-R-B2) can be seen where the B19'-R transformation peak is higher than R-B2 because the energy of the R phase is closer to the austenite phase.

Also during the cooling cycle, three peaks can be seen in this curve. The aggregation of Ni_4Ti_3 precipitates in sites with disorders results in a two-stage transformation. By comparison, in locations without

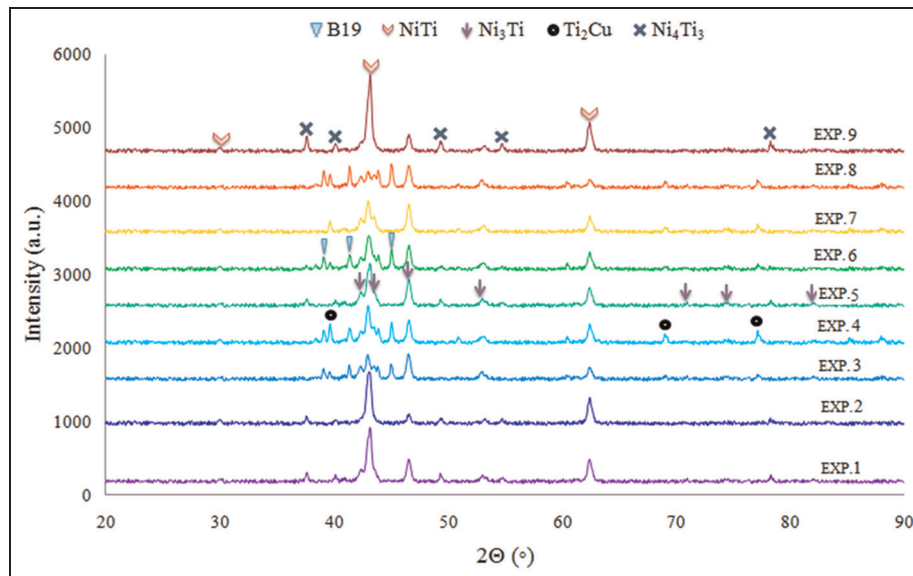


Figure 2. XRD patterns of produced samples (experiments were carried out according to the input parameters of Table 2). XRD: X-ray diffraction.

precipitates, a typical one-stage transformation is observed. Additionally, differing compositions at each site lead to different transformation temperatures.

In the XRD patterns in Figure 2 for specimens 1, 5 and 9 (0% Cu), the Ni_4Ti_3 phase is recognisable. By increasing the sintering time (4, 7 and 10 h) in these specimens (5, 1 and 9, respectively), the height of the Ni_3Ti peaks was reduced, the amount of NiTi phase was increased, and thus, the amount of Ni in the matrix was increased. Moreover, the existence of more Ni in the matrix results in a drastic reduction in the transformation temperature (Frenzel et al., 2007) and increased amount of Ni_4Ti_3 precipitates, which facilitates the martensitic transformation. Meanwhile, it should be mentioned that according to the results of this work (listed in previous section; Table 6), the milling time and compaction pressure are insignificant processing parameters and so the effect of these parameters is not discussed here.

In Figure 1, for the second experiment, the specimen experiences a one-stage transformation. The presence of less than 5% Cu does not have any special effect on the transformation process, but it can facilitate twinning in austenite and increase the transformation temperature. Moreover, the presence of Cu prevents the formation of Ni_4Ti_3 (Goryczka and Van Humbeeck, 2008). For the third specimen (specimen with 10% Cu), a two-stage transformation of B2-B19-B19' is observed, and the peak height of the first stage is smaller than that of the second stage, consistent with our expectations.

As mentioned previously, the existence of 10 at% Cu in the chemical composition prevents the formation of the Ni_4Ti_3 phase. During the ageing process, formation of Ti_2Cu precipitates facilitates the martensitic transformation and is considered as a proper site for the nucleation of martensite.

By increasing sintering time (Figure 1) in the ninth experiment, as it can be seen, the temperature distance between the sites with two-stage transformation and sites without precipitates increases. Besides the type of transformation, the phase distribution and transformation temperature can influence the recoverable strain amount.

Among all the stress–strain curves of Figure 3, it can be seen that almost the least amount of upper stress is related to third specimen, which can be due to easier transformation of B2-B19 in comparison with B2-B19'. Also, creation of Ti precipitates through ageing process provides preferred sites for martensite nucleation, which in turn, facilitates the austenite transformation.

Furthermore, for the third experiment of Figure 1, finishing temperature of austenitic transformation (A_f) is 27 °C, while the temperature of the testing environment is 25 °C; it means that the austenite phase stability is rather low in this temperature and so least amount of stress is required for austenite transformation, as it can be seen in Figure 3.

By evaluating the XRD results using X'Pert software (Table 7), different approximate weight percents of NiTi and $(\text{Ni}, \text{Cu})_3\text{Ti}$ for nine experiments can be obtained. It can be seen that by increasing the ratio of NiTi to $(\text{Ni}, \text{Cu})_3\text{Ti}$, the recoverable strain has increased (Figure 4).

As it mentioned earlier in the optimisation section, more amount of difference between the maximum and minimum of the grey relational grades for each parameter, as listed in Table 6, represents the stronger effect of that parameter on the output response. So from this point of view, the Cu (at.%) and sintering time are more significant than compaction pressure and milling time which accommodates with our expectations. As

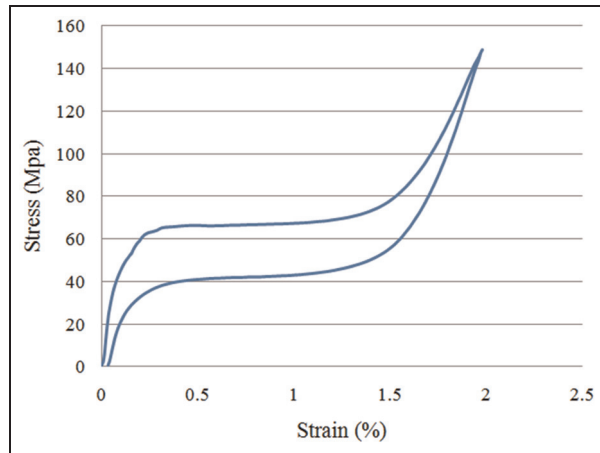


Figure 3. Stress–strain curve for the third experiment of Table 2 (milling time = 36 h, compaction pressure = 900 MPa, sintering time = 4 h and Cu (at.%) = 10).

Table 7. X'Pert results for approximate amount of unwanted (Ni, Cu)₃Ti phase.

No.	(Ni, Cu) ₃ Ti	NiTiC	NiTi/(Ni, Cu) ₃ Ti	ε
1	22	73	3.32	0.95
2	19	72	3.79	1.07
3	12	66	5.50	1.22
4	10	75	7.50	1.45
5	35	61	1.71	0.75
6	17	74	4.35	1.20
7	33	62	1.88	0.78
8	19	68	3.58	1.10
9	23	66	2.87	0.85

mentioned previously, Cu plays different roles in composition. It seems that formation of (Cu, Ni)₃Ti causes local change in the chemical composition, and by decreasing the Ni and Cu content in austenite phase, the martensitic transformation temperature increases. Also for sintering time, as mentioned by Zhu et al. (2004) and Green et al. (1997), in the early stages of sintering, formation of fine pores occurs due to the faster diffusion rate of Ni and Cu than Ti according to the Kirkendall effect, and in the next stages, collection and shrinkage of original pores occur. It seems that for low sintering time (4 h), formation of new fine pores is dominant and for long sintering time (7 h, 10 h), shrinkage of original pores determines the final porosity of microstructure, which in turn impacts recoverable strain of samples. On the other hand, with regard to compaction pressure, as Zhu et al. (2005) concluded in their work, probably due to the work hardening, deformation of powders was difficult and so it is expected that the use of higher pressures may not have much impact on output responses. Although milling time is expected to be one of the important factors in this

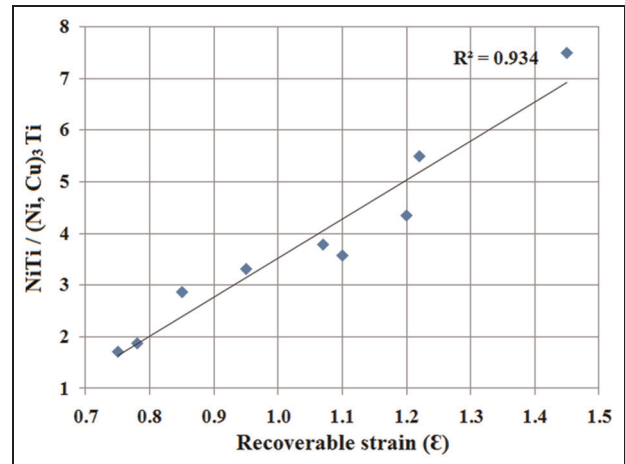


Figure 4. Effect of unwanted phases on recoverable strain.

process, probably due to the selected range of time for milling (20–54), changing of milling time in this area shows no significant effect on the output responses.

To verify the influence of the optimal parameter combination on the output parameters (A_f and ε), a confirmation experiment was carried out. The parameter A_f was 38 °C and ε was 1.7, whereas the combination of experiment 4 (most amount in Table 5) had A_f as 32 °C and ε at 1.45, demonstrating 18.7% and 17.2% improvements for A_f and ε , respectively. The DSC and stress–strain curves for confirmation experiment can be seen in Figure 5.

Conclusion

This research focused on the optimisation of parameters for PM processing to produce NiTiCu specimens. For good shape memory function in biomedical applications, it is ideal to have an alloy with transformation temperature around the body temperature. So due to the results of this work for A_f and ε , the object of this optimisation was to maximise both A_f and ε .

Since various parameters are involved in production of specimens by PM methods, use of experimental design in such cases can be very useful, but usually classical experimental design methods are complicated, time-consuming and costly. Therefore, in this work, by using Taguchi orthogonal arrays, the number of experiments reduced, and due to limitation of Taguchi method for multi-objective optimisation, a GRA was used for optimisation of object responses. This approach converts a multiple response optimisation problem into a single response optimisation called grey relational grade. Using this method, the optimisation process can be significantly simplified. The results of our analysis revealed that the best levels for optimal performance can be obtained by setting the milling time at 20 h, the compaction pressure at 900 MPa, the

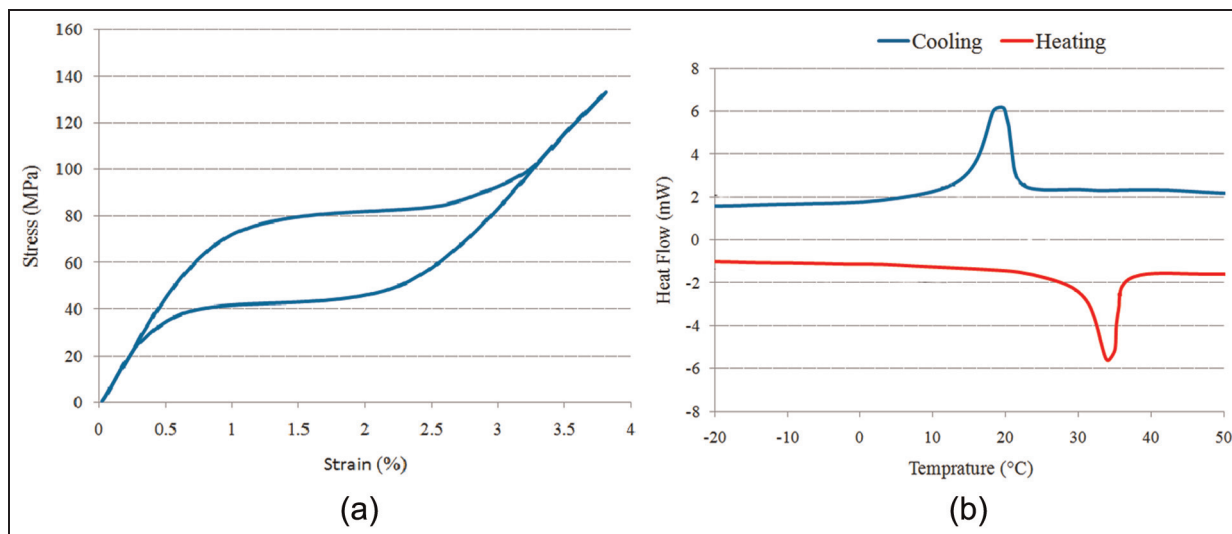


Figure 5. (a) Stress–strain curve and (b) DSC curve for confirmation experiment (milling time = 20 h, compaction pressure = 900 MPa, sintering time = 10 h and Cu (at.%) = 10).

sintering time at 10 h and Cu at 10%. Our results showed that the sintering time and the atomic percentage of Cu are the most significant parameters and have stronger effect on responses than milling time and compaction pressure. The results of our confirmation experiment revealed an 18.7% and 17.2% improvement for A_f and ε , respectively.

Declaration of conflicting interests

The authors declare that there is no conflict of interest.

Funding

This research was funded by the central office of ACECR (Academic Centre for Education, Culture and Research).

References

- Arciniegas M, Aparicio C, Manero JM, et al. (2007) Low elastic modulus metals for joint prosthesis: tantalum and nickel–titanium foams. *Journal of the European Ceramic Society* 27: 3391–3398.
- Bram M, Ahmad-Khanlou A, Heckmann A, et al. (2002) Powder metallurgical fabrication processes for NiTi shape memory alloy parts. *Materials Science and Engineering A* 337: 254–263.
- Chu CL, Chung CY, Lin PH, et al. (2004) Fabrication of porous NiTi shape memory alloy for hard tissue implants by combustion synthesis. *Materials Science and Engineering A* 366: 114–119.
- Chung CY, Chu CL and Wang SD (2004) Porous TiNi shape memory alloy with high strength fabricated by self-propagating high-temperature synthesis. *Materials Letters* 58: 1683–1686.
- Deng JL (1982) Control problems of grey systems. *Systems & Control Letters* 1: 288–294.
- Deng JL (1989) Introduction to grey system theory. *Journal of Grey System* 1: 1–24.
- Elahinia MH, Hashemi M, Tabesh M, et al. (2012) Manufacturing and processing of NiTi implants: a review. *Progress in Materials Science* 57: 911–946.
- Frenzel J, Zhang Z, Somsen C, et al. (2007) Influence of carbon on martensitic phase transformations in NiTi shape memory alloys. *Acta Materialia* 55: 1331–1341.
- Goryczka T and Van Humbeeck J (2008) NiTiCu shape memory alloy produced by powder technology. *Journal of Alloys and Compounds* 456: 194–200.
- Green SM, Grant DM and Kelly NR (1997) Powder metallurgical processing of Ni–Ti shape memory alloy. *Powder Metallurgy* 40: 43–47.
- Guoxin H, Lixiang Z, Yunliang F, et al. (2008) Fabrication of high porous NiTi shape memory alloy by metal injection molding. *Journal of Materials Processing Technology* 206: 395–399.
- Khalifehzadeh R, Forouzan S, Arami H, et al. (2007) Prediction of the effect of vacuum sintering conditions on porosity and hardness of porous NiTi shape memory alloy using ANFIS. *Computational Materials Science* 40: 359–365.
- Lagoudas DC and Vandygriff EL (2002) Processing and characterization of NiTi porous SMA by elevated pressure sintering. *Journal of Intelligent Material Systems and Structures* 13: 837–850.
- Li B-Y, Rong L-J and Li Y-Y (1998) Porous NiTi alloy prepared from elemental powder sintering. *Journal of Materials Research* 13: 2847–2851.
- McNeese MD, Lagoudas DC and Pollock TC (2000) Processing of TiNi from elemental powders by hot isostatic pressing. *Materials Science and Engineering A* 280: 334–348.
- Maziarz W, Dutkiewicz J, Van Humbeeck J, et al. (2004) Mechanically alloyed and hot pressed Ni–49.7Ti alloy showing martensitic transformation. *Materials Science and Engineering A* 375: 844–848.
- Neves F, Fernandes FMB, Martins I, et al. (2011) Parametric optimization of Ti–Ni powder mixtures produced by mechanical alloying. *Journal of Alloys and Compounds* 1: 271–274.

- Pilarczyk W, Nowosielski R, Pilarczyk A, et al. (2011) A production attempt of Ni₅₀Ti₅₀ and Ni₅₂Ti₅₂Nb₇ alloys by mechanical alloying method. *Archives of Materials Science and Engineering* 47: 19–26.
- Roy RK (2010) *A Primer on the Taguchi Method*. 2nd ed. Dearborn, MI: Society of Manufacturing Engineers.
- Ryan G, Pandit A and Apatsidis DP (2006) Fabrication methods of porous metals for use in orthopaedic applications. *Biomaterials* 27: 2651–2670.
- Sadrnezhaad SK and Selahi AR (2004) Effect of mechanical alloying and sintering on Ni-Ti powders. *Materials and Manufacturing Processes* 19: 475–486.
- Schöller E, Krone L, Bram M, et al. (2005) Metal injection molding of shape memory alloys using prealloyed NiTi powders. *Journal of Materials Science* 40: 4231–4238.
- Tay KM and Butler C (1999) Methodologies for experimental design: a survey, comparison and future predictions. *Quality Engineering* 11(3): 343–356.
- Terayama A and Kyogoku H (2010) Shape memory characteristics of the P/M-processed Ti–Ni–Cu alloys. *Materials Science and Engineering A* 527: 5484–5491.
- Zhang N, Babayan Khosrovabadi P, Lindenhovius JH, et al. (1992) TiNi shape memory alloys prepared by normal sintering. *Materials Science and Engineering A* 150: 263–270.
- Zhao Y, Taya M, Kang Y, et al. (2005) Compression behavior of porous NiTi shape memory alloy. *Acta Materialia* 53: 337–343.
- Zhu SL, Yang XJ, Fu DH, et al. (2005) Stress–strain behavior of porous NiTi alloys prepared by powders sintering. *Materials Science and Engineering A* 408: 264–268.
- Zhu SL, Yang XJ, Hu F, et al. (2004) Processing of porous TiNi shape memory alloy from elemental powders by Ar-sintering. *Materials Letters* 58: 2369–2373.